Journal of Polymer Research (2023) 30:387
https://doi.org/10.1007/s10965-023-03770-y

ORIGINAL PAPER

Mechanically robust room-temperature self-healing waterborne polyurethane with antimicrobial properties constructed through multiple dynamic bonds

Yuan Wang[1] · Liang Chen[1] · Pingping Jiang[1] · Pingbo Zhang[1] · Yanmin Bao[2] · Xuewen Gao[2] · Jialiang Xia[2]

Received: 10 May 2023 / Accepted: 8 September 2023 / Published online: 20 September 2023

Abstract

In this study, 2,6-diacetylpyridine dioxime was synthesized from 2,6-diacetylpyridine and hydroxylamine hydrochloride as raw materials and bonded into the molecular chain of waterborne polyurethane as an alcohol chain extender, Subsequent addition of Cu^{2+} interacted with the Schiff base structure in the WPU molecular chain to generate room-temperature self-healing polymeric materials with multiple dynamic bonds based on ligand bonds, oxime carbamates, and hydrogen bonds. Due to the synergistic effect of multiple dynamic bonds, DWPU-$Cu_{0.25}$ exhibited excellent mechanical properties (tensile strength of 11.9 MPa and elongation at break of 1620%) and excellent room temperature self-healing ability (healing efficiencies of 89.1% and 95.8% for elongation at break and tensile strength, after 72 h of room temperature healing). Additionally, antibacterial experiments showed that DWPU-Cu films can release copper ions and create antibacterial zones around polyurethane films, demonstrating their use in the field of antibacterial coatings. By introducing covalent bonds and non-covalent dynamic bonds into the waterborne polyurethane to improve the healing ability of the material, and this internal self-healing method avoids the disadvantages of the external self-healing method, such as irreversibility, complex operation and poor compatibility. This self-healing mechanism based on the dynamic bond inside the material can not only realize repeated self-healing, but also have excellent basic properties, and can also expand other functions on the basis of self-repair, and realize the application of multifunctional materials.

Keywords Waterborne polyurethane · Self-healing · Antimicrobial · Metal-ligand

Introduction

Green and ecologically friendly materials have attracted a lot of interest in the context of growing environmental concerns, with the development of waterborne polyurethanes receiving a lot of attention. Traditional polyurethanes are restricted because toxic and harmful volatile organic compounds (VOCs) will be released during the production process, and waterborne polyurethanes (WPU), which use water as the dispersion medium, are considered an alternative to traditional solvent-based polyurethanes [1–3]. WPU material has properties such as low-temperature resistance, flexibility, abrasion resistance, and corrosion resistance, which make it widely used in adhesives [4], water-based inks [5], textile composites [6],and biological materials [7]. However, WPU materials are susceptible to external irritation during use, and cracks will form inside them will reduce the durability of polymeric materials. Inspired by the ability of plants and animals in nature to spontaneously repair wounds,

Highlights
1. Room temperature self-healing waterborne polyurethane based on coordination bonds, oxime carbamates and hydrogen bonds.
2. Waterborne polyurethane film with antibacterial properties against Escherichia coli and Staphylococcus aureus.
3. A novel oxime chain extender 2,6-diacetylpyridine dioxime prepared by the reaction of 2,6-diacetylpyridine with hydroxylamine hydrochloride.
4. Waterborne polyurethane excellent mechanical properties gived by the synergy of various dynamic bonds.

✉ Pingbo Zhang
pingbozhang@126.com

[1] Key Laboratory of Synthetic and Biological Colloids, School of Chemical and Material Engineering, Ministry of Education, Jiangnan University, Wuxi 214122, P. R. China

[2] Jiangsu Caihua Packaging Group Company, Kunshan 215321, P. R. China

the emerging concept of self-healing provides an effective way for self-healing of microcracks [8]. Therefore, introducing self-healing features in WPUs effectively improves their durability and reduces maintenance costs.

Currently, there are two strategies to achieve self-healing ability: external self-healing and internal self-healing. external self-healing is accomplished by releasing healing agents into matrix micro-containers. However, this method has several limitations, including a loss of healing ability when the healing agent is depleted, the complexity of the operation, and poor compatibility [9]. Internal self-healing is achieved by reversible reactions of dynamic covalent and non-covalent bonds. Dynamic non-covalent bonds mainly include hydrogen bonds [10, 11],metal-ligand coordination [12, 13], ionic interactions [14, 15], π-π stacking [16, 17],and host-guest interactions [18, 19], and also dynamic covalent bonds mainly include Diels-Alder (DA) reactions [20, 21], disulfide bonds [22, 23], borate ester bonds [24, 25],and oxime carbamates [26, 27].Intrinsic self-healing mainly has the advantages of a simple preparation process, no need for repair agents, and repeatable healing. Since most waterborne polyurethane materials are required to be used at room temperature, we need to design polyurethane materials that can heal at room temperature. Self-healing requires high external conditions due to the weak kinetic nature of covalent bonds and the poor diffusivity of polymer chains [28], while the most effective method for room temperature healing is to incorporate dynamic non-covalent interactions.

Both hydrogen and ligand bonds are typically dynamic non-covalent bonds. hydrogen bonds are weakly dynamic and have much lower energies than covalent bonds. Ligand bond strengths are intermediate between van der Waals interactions and covalent bonds, and ligand bonds can be modulated over a considerable range due to a variety of readily available ligands and metal ions, which makes them very attractive in the field of room temperature self-healing materials. The synergy of covalent and non-covalent bonds to form multiple dynamic cross-linked network structures, inspired by the cross-linking mechanisms of weak and strong bonds, is a research trend to study room-temperature self-healing with high mechanical properties. Zhang et al. [29] synthesized room-temperature self-healing thermoplastic polyurethanes (TPUs) with multiple hydrogens, reversible disulfide, and coordination bonds. The prepared elastomers exhibited a tensile strength of more than 16.1 MPa and a tensile strain of 771%, and the multiple dynamic bonds conferred high self-healing efficiency (94%) to the elastomers within 24 h at room temperature. Wang et al. [30] designed a poly-self-healing polyurethane including disulfide bonds, oxime-carbamate bonds, hydrogen bonds, and coordination interactions.

The Cu^{2+} acts as a ligand center and a catalyst to accelerate the disulfide exchange and oxime-carbamate exchange reactions. Due to the multiple interaction design and Cu^{2+}, the elastomer has an excellent mechanical strength of 19.5 MPa at room temperature and a self-healing efficiency of 83%. Although coordination bonds have been successfully introduced into polyurethane materials to achieve self-healing at room temperature, the preparation process requires a large amount of toxic or environmentally harmful organic solvents. The study of waterborne polymeric materials with excellent mechanical properties and self-healing at room temperature, especially high-performance environmentally friendly waterborne polyurethanes based on strong and weak bond synergies, is still in need of further research. In addition, WPU with a single self-healing function cannot meet people's production and living needs well. Therefore, giving WPU more functions, such as antibacterial properties, is important to expand its application scope and increase its added value.

By introducing covalent bonds and non-covalent dynamic bonds into the waterborne polyurethane to improve the healing ability of the material, and this internal self-healing method avoids the disadvantages of the external self-healing method, such as irreversibility, complex operation and poor compatibility. This self-healing mechanism based on the dynamic bond inside the material can not only realize repeated self-healing, but also have excellent basic properties, and can also expand other functions on the basis of self-repair, and realize the application of multifunctional materials. Here, based on the synergistic cross-linking mechanism of strong and weak bonds and certain specific biological properties of metal ions, we synthesized a mechanically robust room-temperature self-healing waterborne polyurethane material with certain antibacterial properties. It provides some reference value for the study of multifunctional and environmentally friendly waterborne polyurethane coatings.

Experiment

Materials

Isophorone diisocyanate (IPDI, 99%), hydroxylamine hydrochloride ($NH_2OH{\cdot}HCl$, 99%), and 2,6-diacetylpyridine (98%) are purchased from Shanghai Titan Technology Co. Polytetrahydrofurandiol (PTMG, Mn = 1000), 2, 2-bis(hydroxymethyl)propionic acid (DMPA, 99%) from Aladdin (Shanghai) Co. Acetone (99%), N-methyl pyrrolidone (NMP, 99%), triethylamine (TEA, 99%), stannous octanoate (99%), sodium acetate (NaOAc, 99%), copper chloride dihydrate ($CuCl_2{\cdot}2H_2O$, 99%), tryptone (99%), agar powder (99%), yeast powder (99%), sodium chloride (99%) were purchased from Shanghai Sinopharm Chemical Reagent Co.

Synthesis of 2,6-diacetylpyridine dioxime

Deionized water and ethanol were combined in a specific mass ratio in a 250 ml three-necked flask. Next, 3.26 g of 2,6-diacetylpyridine, 5.21 g of hydroxylamine hydrochloride, and 8.20 g of sodium acetate were added to the flask one at a time. The mixture was then heated to 90 °C and refluxed for 2.5 h. It was then cooled to room temperature, and the crude product was produced by filtration under decreased pressure and washed at least five times with deionized water. Finally, the cleaned product was dried in a vacuum drying oven at 60 °C for 24 h to create a white powder sample. Figure 1 is a schematic diagram of the synthesis of 2,6-diacetylpyridine doxime.

Synthesis of DWPU

The preparation process for DWPU consists of several steps. Firstly, IPDI and PTMG were weighed and added to a 100ml three-neck flask with a stirring magnet and reflux device. Adjust the temperature of the oil bath at 80 ± 2 °C, keep the temperature reaction for 1 h, then add NMP mixed solution with DMPA dissolved in the flask, stir the system for 5 min and then add two drops of stannous octanoate, after 1 h reaction, add 10ml acetone to adjust the viscosity of the system to avoid gelation, continue the reaction for 2 h. The system was cooled down to 60 °C, and 2,6-diacetylpyridine dioxime was added to continue the reaction for 1.5 h. The system temperature was adjusted to 50 °C, and triethylamine was added to neutralize the reaction for 30 min, and then the reaction was cooled to room temperature. Place the three-necked flask in an ice-water bath set at 0–5 °C, use mechanical stirring with a speed of 1800–1900 rpm/min, add deionized water fast, shear emulsify for 1 h, and then use a rotary evaporator to spin evaporate at 50 °C for 30 min to produce a waterborne polyurethane emulsion with 20% solid content. The prepared emulsions were cast in a PTFE film tool, dried at room temperature for 48 h, and then transferred to a vacuum drying oven at 60 °C for 24 h. All films were stored in the desiccator before characterization.

Synthesis of DWPU-Cu

To synthesize the DWPU-Cu, the other synthetic procedures were the same as for the DWPU emulsion, except that the deionized water used alone was replaced by an aqueous solution obtained by dissolving a specific amount of $CuCl_2{\cdot}2H_2O$ for the emulsification process. The schematic diagram of the synthesis is shown in Fig. 2, and the formulation table is shown in Table S1.

Characterization

The FTIR spectra of the samples were detected by an infrared spectrometer (Nicolet 6700, Thermo Fisher Scientific Co, USA) using a DLaTGS detector in the wave number range of $4000-500\ cm^{-1}$ with an average of 32 scans and a resolution of $4\ cm^{-1}$.

The ^{1}H-NMR spectrum of 2,6-diacetylpyridine was studied by Bruker instrument (Avance 400, Germany). A 5–10 mg sample was placed in an NMR tube and DMSO-d6 was chosen as the solvent.

A UV spectrophotometer TU-1950 (Beijing Pu-Analysis General Instrument Co., Ltd.) can be used to perform UV-visible spectroscopy in the range of 800 to 200 nm for each polyurethane solution at a concentration of 0.1 mg/ml.

The chemical composition and valence states of different elements in polyurethane composite films were investigated using an Axis supra-type X-ray photoelectron spectrometer.

The particle size and distribution of the emulsions were studied using a zeta potential and nanoparticle size analyzer from Brookhaven, USA (Zeta PALS). The concentration of the emulsions was diluted to 0.1wt% with deionized water, and the samples were tested at 25 °C with a laser scattering angle of 90°.

OCA40 Optical contact angle measuring instrument (Beijing Dongfang Defei Instrument Co, Ltd, China) was used to measure the surface hydrophobicity of polyurethane films. Deionized water was selected as probe liquid, and three parallel tests were carried out at room temperature, and the results were expressed as mean values.

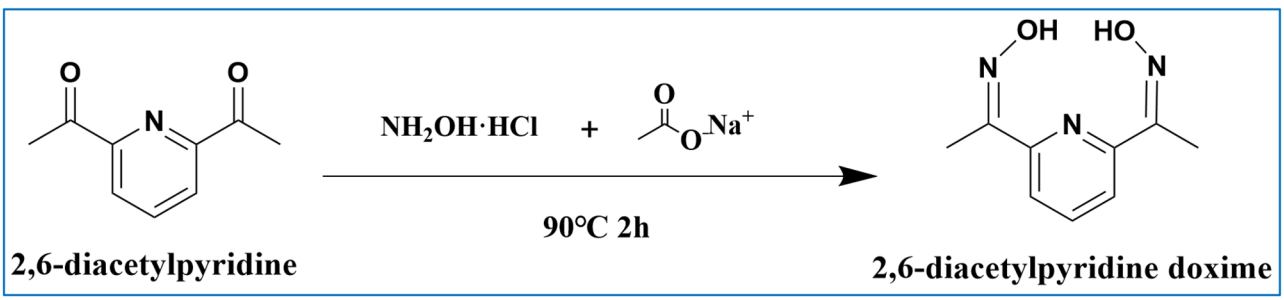

Fig. 1 Synthetic route of 2,6-diacetylpyridine dioxime

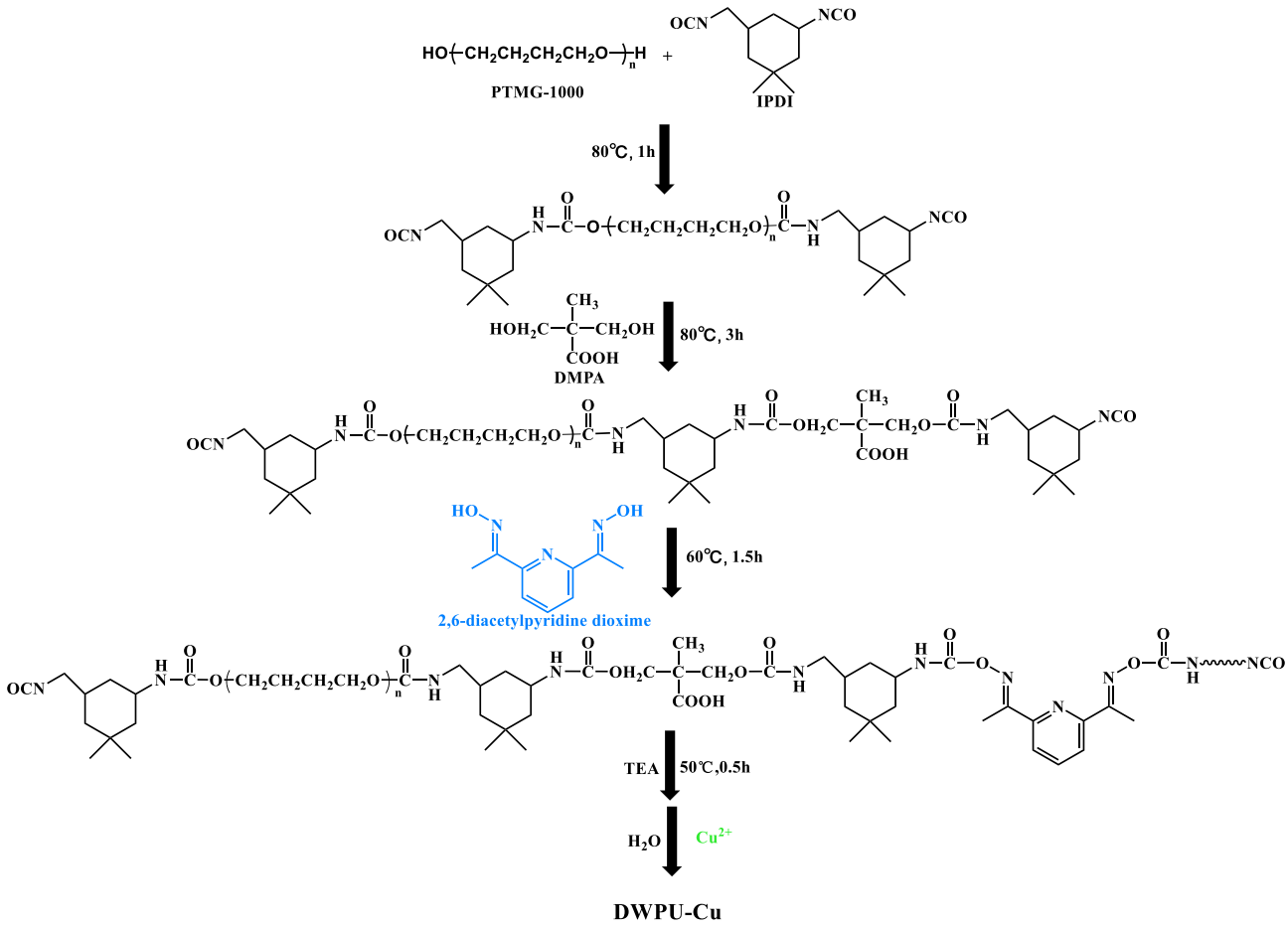

Fig. 2 Schematic diagram of DWPU-Cu.

The mechanical properties of the films were determined at room temperature using a film tensile strength tester (XLW PC, Jinan Blue Electromechanical Technology Co, Ltd, China). Samples (dumbbell-shaped, width 2 mm, length 10 mm) were prepared and tested at a 50 mm /min displacement rate.

To simulate cracks, the films were scratched with a razor blade to about 50% of the sample thickness. The scratches' healing process was monitored in real-time by hot-stage polarized light microscopy (POM, Axio Imager A2POL, Germany) with a magnification of 50.

To evaluate the self-healing efficiency and to quantitatively characterize the mechanical properties and self-healing efficiency of the samples, the samples (dumbbell-shaped, 2 mm in width and 10 mm in length) were cut into two halves with a razor blade, and then the cut surfaces were spliced together for about 15 s to ensure a tight connection. After healing for different times at room temperature, the mechanical properties of the healed DWPU-Cu were measured using a film tensile strength tester at a displacement rate of 50 mm/min at room temperature. The self-healing efficiency (η) of the samples was calculated according to the following equation: the self-healing efficiency (η) of the studied specimens was defined as [29]:

$$\eta = \left[\sigma(\text{heal})/\sigma(\text{original})\right] \times 100\% \quad (1)$$

σ(heal) and σ(original) are the tensile strength and tensile strain of the repaired specimen, the original specimen, respectively.

The antibacterial properties of the modified polyurethane films were determined by a bacterial inhibition test. All experimental equipment was sterilized before the experiment. 40μL of activated Staphylococcus aureus (S. aureus, Gram-positive, ATCC 292,213) and Escherichia coli (E. coli, Gram-negative, ATCC 25,922) were evenly applied to the solid medium substrate employing a coating stick, and the WPU coating was made into a circle with a diameter of 1 cm and placed on the solid on the medium and kept in a constant temperature incubator at 37 °C for 24 h. The samples were then observed for bacterial growth around the samples.

Results and discussion

Structure of 2,6-diacetylpyridine dioxime

FTIR and ^{1}H-NMR spectra were used to confirm the chemical structures of 2,6-diacetylpyridine dioxime. Fig. S1 displays the IR spectra of 2,6-diacetylpyridine and 2,6-acetylpyridine dioxime. According to the figure, the ketone group has completely reacted because 2,6-acetylpyridine dioxime lacks the 2,6-diacetylpyridine's distinctive peak at 1700 cm^{-1}, which is a stretching vibrational peak belonging to the C = O group. In addition, a weak absorption peak was observed at 3223 cm^{-1}, which corresponded to the stretching vibration peak of -OH. Fig. S2 shows the NMR hydrogen spectrum of the sample, which corresponds to the H-proton peak on -OH at position a on 2,6-diacetylpyridine dioxime at 11.5 ppm. two absorption peaks at 7.81 ppm belong to the hydrogen proton peaks on the pyridine ring's unsaturated carbon of b and c. the obvious absorption peak at 2.5 ppm corresponds to the hydrogen proton peak on $-CH_3$ at position d 2,6-diacetylpyridine dioxime. Based on the above structural characterization, it was demonstrated that 2,6-diacetylpyridinedioxime was successfully synthesized [31].

Structural analysis of waterborne polyurethane

Figure 3(a) shows the IR spectra of DWPU and DWPU-Cu films. The figure shows that strong absorption peaks appear near 3314 cm^{-1} and 1700 cm^{-1} for all samples, which correspond to the -NH- and -C = O stretching vibration peaks of urethane molecular structure, respectively. The characteristic peaks at 2940 cm^{-1} and 2854 cm^{-1} are $-CH_2$ and -CH- groups, respectively. The absorption band near 1535 cm^{-1} belongs to the bending vibration peak of -NH-, and no absorption band was observed between 2200 and 2300 cm^{-1}, which can prove that the -NCO group has been fully reacted and the waterborne polyurethane was successfully synthesized. The sample showed an absorption peak at 985 cm^{-1}, which corresponds to the N-O bond in the oxime-carbamate bond, where the reactive group is formed by the reaction of the hydroxyl group in the acetylpyridine dioximide with -NCO [32]. In addition, the absorption peak of the sample at 853 cm^{-1} corresponds to the out-of-plane bending vibration of C-H on the pyridine ring. All of the above indicates the synthesis of 2,6-diacetylpyridinedioxime as one of the raw materials in the polyurethane molecular chain.

UV-Vis absorption spectroscopy and XPS spectroscopy are used to evaluate DWPU and DWPU-Cu to demonstrate the effective complexation of Cu^{2+} with Schiff bases in polyurethane. As shown in Fig. 3b, DWPU showed an absorption peak near 316 nm. This is because the unique conjugated Schiff base structure in DWPU [33]. The absorption peak of this structure in DWPU-$Cu_{0.25}$ is shifted to nearly 367 nm, and this red-shift phenomenon can be attributed to the ligand field jump caused by the complexation of Cu^{2+} with the Schiff base. Cu before and after coordination was analyzed using narrow XPS in Fig. S3. No peaks belonging to Cu were detected in the XPS spectra of DWPU. As shown in Fig. S3(b), the presence of Cu 2p peaks at 930.4 eV and 933.3 eV of DWPU-$Cu_{0.25}$ proves the formation of copper complexes of Schiff base ligands. The presence of oscillatory peaks at 941.2 eV and 949.5 eV indicates the presence of partially coordinated copper ions [34].

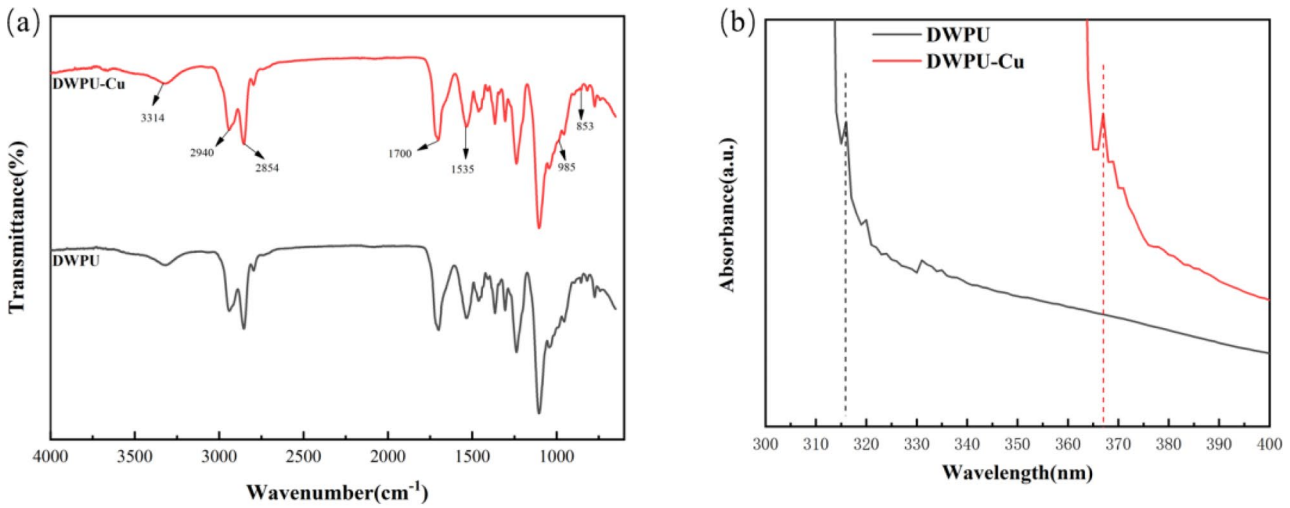

Fig. 3 **a** FTIR spectra, **b** UV-visible absorption spectra of DWPU and DWPU-$Cu_{0.25}$

Particle size distribution of water-based polyurethane emulsions

Figure 4 shows the particle size distribution of DWPU and DWPU-Cu emulsions. The average particle sizes of DWPU, DWPU-$Cu_{0.25}$, and DWPU-$Cu_{0.5}$ are 33.5 nm, 72.2 nm, and 108.4 nm, respectively. The polydispersity indexes (PDI) are 0.209, 0.225, and 0.112, respectively. The above data show that all modified polyurethanes can be uniformly dispersed in deionized water. Usually, the particle size of WPU emulsions is affected by chain stiffness, hydrophilic groups, the cross-linked structure of the polymer, and emulsification conditions [35]. Among the above factors, the cross-linked structure has an intrinsic effect on the viscosity and stability of the emulsion. The particle size of the polyurethane emulsions increased with the increase in copper ion content. This is mainly caused by the influence of Cu^{2+}, which can form coordination bonds with the Schiff base structure in the polymer molecular chain, further promoting cross-linking and cohesion between the polyurethane chains, resulting in a larger average particle size of the emulsion [36].

Hydrophilic analysis of composite film surface

Static water contact angle (CA) determination is an important parameter that has studied the hydrophilicity and hydrophobicity of the composite film surface, and Fig. 5 shows the water contact angle data for different polyurethane composite films. The contact angles of DWPU, DWPU-$Cu_{0.25,}$ and DWPU-$Cu_{0.5}$ are 73.6°, 77.7°, and 75.5 °C, respectively, according to the figure. This is primarily because when a certain amount of Cu^{2+} is added to cross-link with the coordination's Schiff base, it blocks some of the hydrophilic groups in the polyurethane's molecular chain and prevents water molecules from dispersing into the material's interior, increasing the contact angle. Excessive copper ions alter the way that polyurethane molecules are arranged, which causes more phase mixing, more water permeability, and a smaller water contact angle [37].

Thermogravimetric analysis

The thermal weight loss curve (TGA) of the DWPU film is shown in Fig. 6, and the temperature values corresponding to the 5% weight loss and 10% weight loss for all samples are listed in Table 1. Usually, the polyurethane membranes exhibit a relatively low thermal stability due to the presence of the labile carbamate groups. All the samples mainly showed two stages of during the thermal decomposition process [38]. The first stage was at 150–350℃, which was attributed to the production of isocyanates, carbon dioxide, alcohols, primary amine, and secondary amines. The second stage is at 350–450 °C . At this stage, the WPU sample decomposes sharply and the carbon chain skeleton

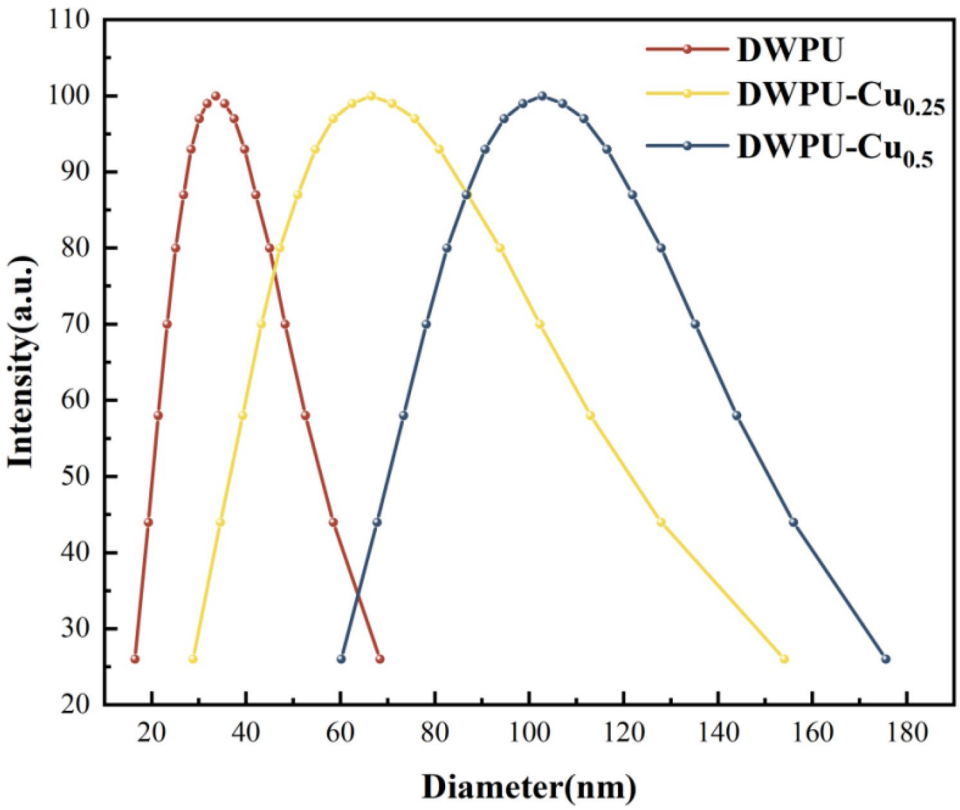

Fig. 4 Particle size distribution of water-based polyurethane emulsions

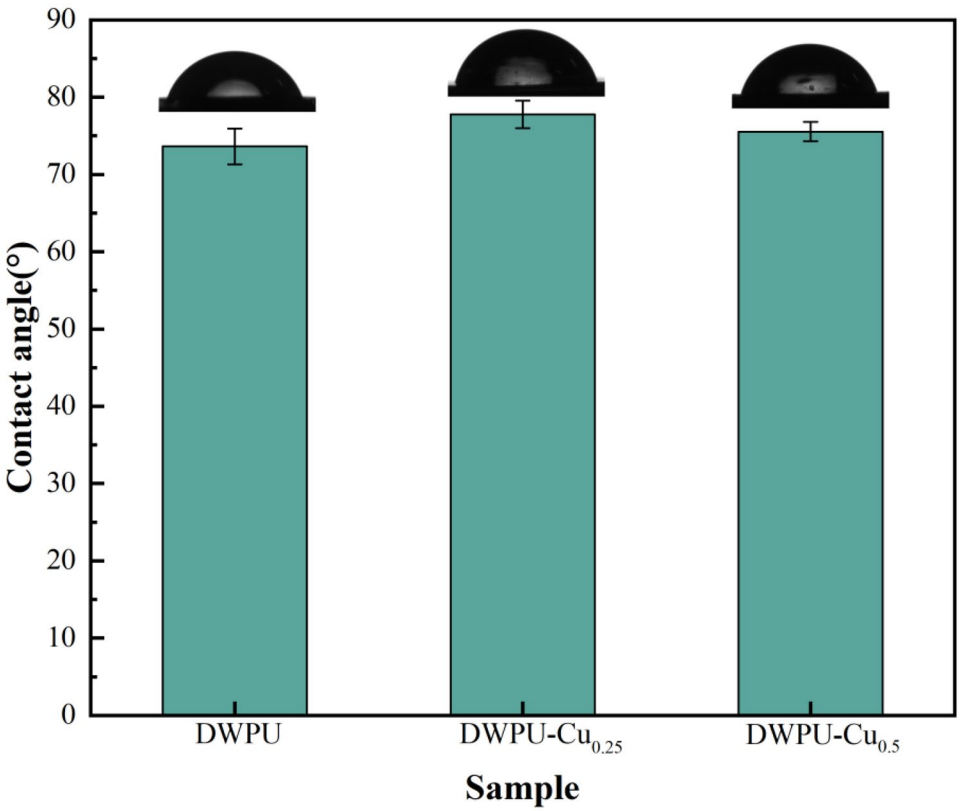

Fig. 5 Contact angle of water-borne polyurethane film

is destroyed, which reflects the characteristics of the degradation of the soft chain segment, that is, the broken chain of the polyether polyol structure. Furthermore, $T_{5\%}$ from Table 1 observed for DWPU-0, DWPU-1, DWPU-1, DWPU-2, DWPU-3 are 291.66 °C, 258.33 °C, 245.66 °C, and 228.33 °C, respectively. Obviously, with the increase of 2,6-diacetylpyridine doxime content, the corresponding $T_{5\%}$ decline, similarly, the $T_{10\%}$ of the sample, the main reason is that WPU degradation behavior by the lowest bond energy, the hard chain segment is more likely to thermal degradation than the soft chain [39], the content of the polyurethane molecular chain increase, so $T_{5\%}$ and $T_{10\%}$ with the increase of 2,6-diacetylpyridine doxime content.

Mechanical properties

To investigate the effect of Cu^{2+} on the mechanical properties of the material, uniaxial tensile tests were conducted. The mechanical properties of the DWPU-Cu composite film are shown in Fig. 7. The tensile strength of DWPU without Cu^{2+} addition was 8.7 MPa and elongation at break was 1435%, but the tensile strength of DWPU-$Cu_{0.25}$ was elevated to 11.9 MPa and elongation at break was 1620% because the complexation of copper ions with Schiff base could enhance its mechanical properties to some extent. Here, copper ions act as cross-linking neutrals, providing multiple cross-linking sites that bind linear polyurethane molecules together, thereby increasing the tensile stress of the material [40]. Due to the coordination complexation of the copper and Schiff base structures, some of the internal polymer chains are folded and, therefore, additional hidden lengths are generated. These hidden lengths are released under stretching by dynamic dissociation and recombination of multiple reversible bonds. The dissipation of large amounts of energy during dissociation and recombination leads to a significant increase in toughness [31, 34]. However, with the addition of copper ions, the tensile strength of DWPU-$Cu_{0.5}$ decreased to 10.5 MPa and the elongation at break decreased to about 1250%. The additional copper ions disrupted the regular arrangement of the molecular chains, leading to greater phase mixing and reduced crystallinity, which were responsible for the reduced mechanical properties of DWPU-$Cu_{0.5}$ [37, 41].

Self-healing property analysis

To verify the effect of the healing ability of the polyurethane material of Cu^{2+}. The self-healing performance of DWPU-Cu was first initially evaluated by a scratch recovery test. A clean razor blade was used to scratch the surface of the composite film with a thickness of approximately 50% of the film thickness and left to heal at room temperature for 24 h. The crack state of the polyurethane film surface after healing at room temperature could be observed by polarized

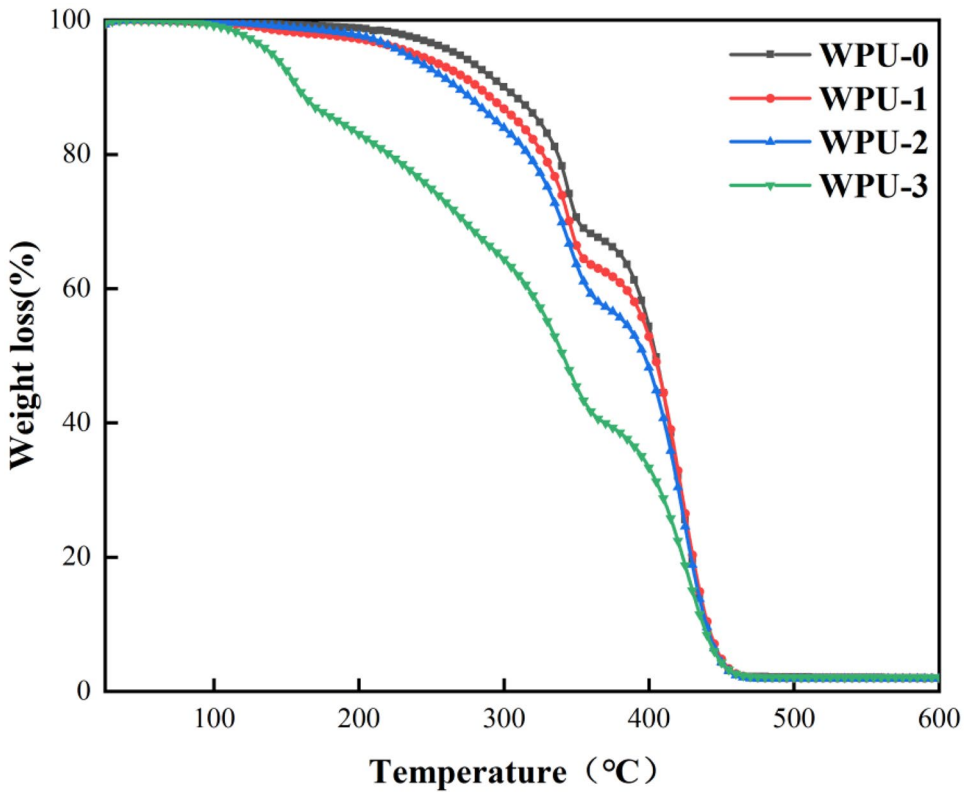

Fig. 6 The TGA curve of DWPU

light microscopy. As shown in Fig. 8, it can be seen from the figure that the cracks on the surfaces of DWPU-$Cu_{0.25}$ and DWPU-$Cu_{0.5}$ disappeared, and DWPU-Cu had excellent spontaneous self-healing ability at room temperature. However, DWPU healed less effectively, and the width of cracks on the surface decreased, but there were relatively clear scratches. To investigate the self-healing properties more visually, we observed the macroscopic self-healing behavior of the DWPU-$Cu_{0.25}$ film. As shown in Fig. 9, the samples were cut and spliced together to heal at room temperature for 72 h. The healed samples could be suspended from a dumbbell piece of 1.25 kg weight. These results provide visual evidence for the self-healing property of DWPU-Cu, thus demonstrating that the addition of Cu^{2+} can effectively enhance the healing ability of the polyurethane material and repair the mechanical properties of the fractured samples.

To further investigate the self-healing behavior of the prepared WPU films systematically, a series of tests on their mechanical properties were carried out. Tensile tests were used to examine the mechanical characteristics of the DWPU-Cu films before and after healing, and the self-healing effectiveness was determined using the tensile strength and elongation at the break before and after repair, respectively. Figure 10(a) and (b) show the mechanical properties of the original samples of DWPU-$Cu_{0.25}$ and DWPU-$Cu_{0.5}$ respectively and the samples healed for different times after severing. Figure 10(c) and (d) summarize the self-healing efficiency of both. The tensile strength and ultimate elongation of DWPU-$Cu_{0.25}$ increased with passing time, as depicted in the figure. After healing at room temperature for 4 h, the DWPU-$Cu_{0.25}$ self-healing efficiency of tensile strength and elongation at break achieved 27.7% and 58.9%, respectively. Tensile strength and elongation at break healing efficiency increased to 89.1% and 95.8%, respectively, after 72 h of healing at room temperature. This may be due to the dissociation of hydrogen, metal-ligand, and oxime-carbamate bonds, which makes the polymer molecular chains on the section diffuse each other, and the deep reorganization of non-covalent and covalent oxime-carbamate bonds over time, forming a new dynamic cross-linked network, whose mechanical properties gradually recovered, and the healing efficiency gradually increased, the principal part of which is shown in Fig. 11 [31, 42, 43].

Compared with DWPU-$Cu_{0.25}$, the healing efficiency of the mechanical properties of DWPU-$Cu_{0.5}$ is relatively low,

Table 1 Thermal decomposition temperature of DWPU

Samples	$T_{5\%}$(°C)	$T_{10\%}$(°C)
DWPU-0	291.66	319.67
DWPU-1	258.33	285.33
DWPU-2	245.66	274.33
DWPU-3	228.33	276.33

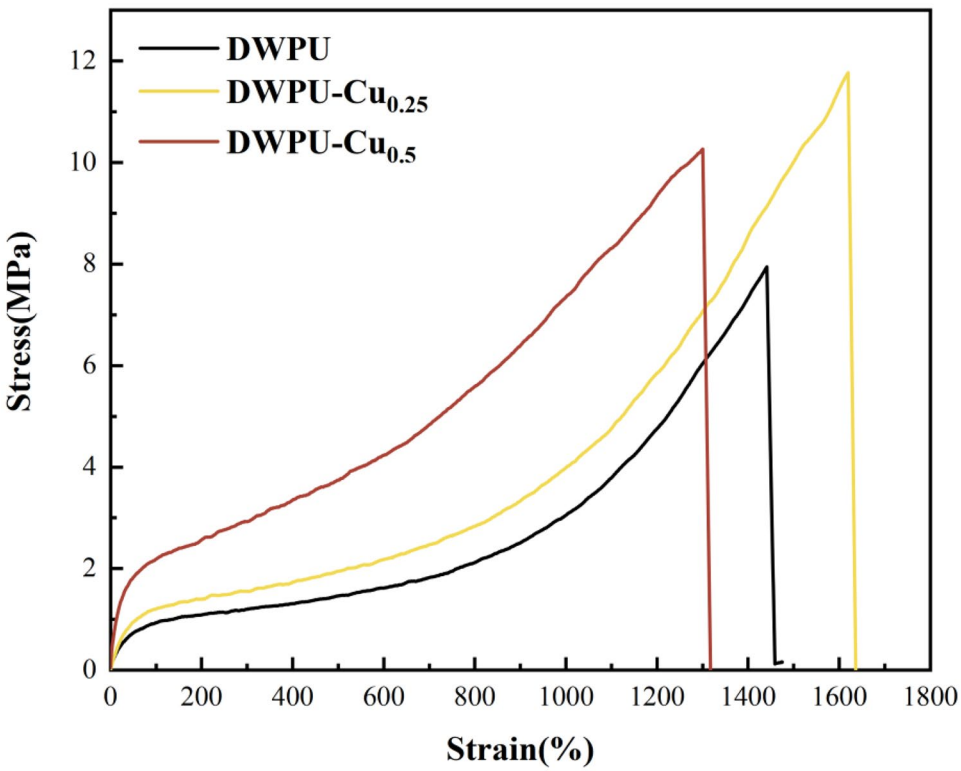

Fig. 7 The mechanical properties of polyurethane film

with the healing efficiency of tensile strength and elongation at the break being 54.8% and 74.8%, respectively, after 72 h of healing at room temperature. It is possible that Excessive Cu^{2+} entry would accumulate in WPU to form defects and thus disrupt the arrangement of molecular chains in polymer. In addition, excessive coordination cross-linking also restricts the mobility of molecular chains and hinders the diffusion of molecules at the fracture surface, both of which lead to a decrease in the healing efficiency of the sample [35, 40, 44].

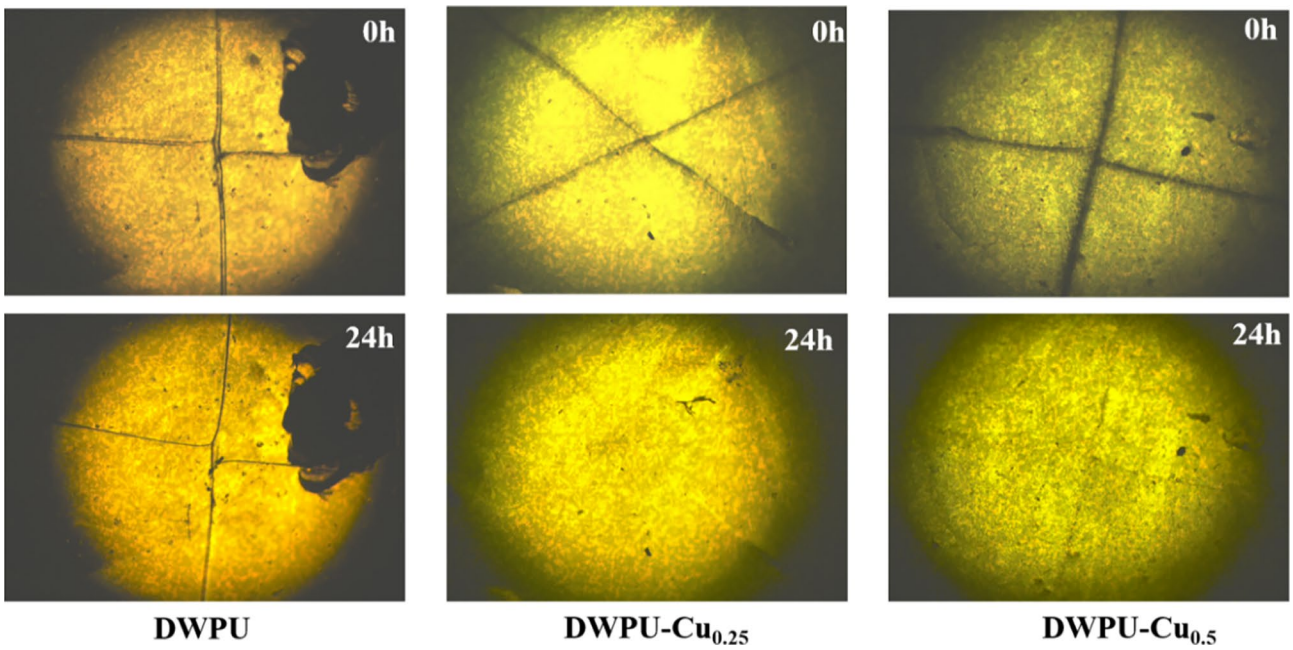

Fig. 8 POM images of the self-healing process of the crack on the polyurethane film

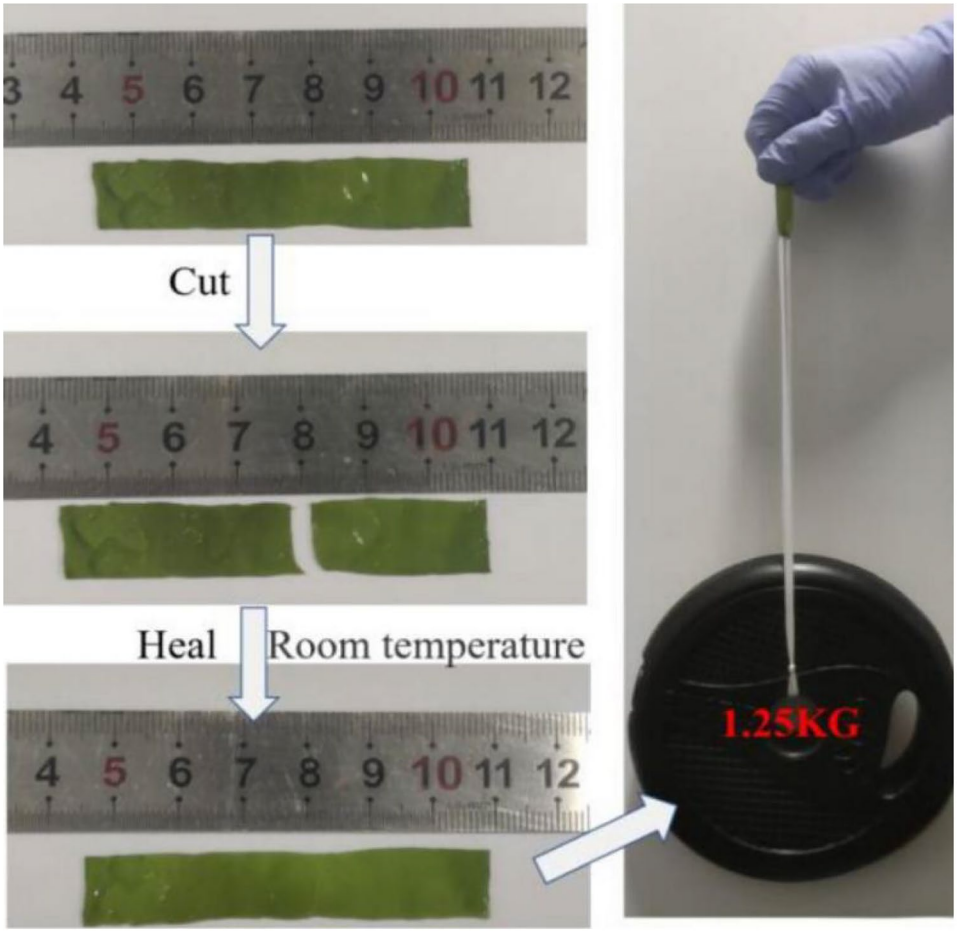

Fig. 9 Self-healing behavior of DWPU-$Cu_{0.25}$ film

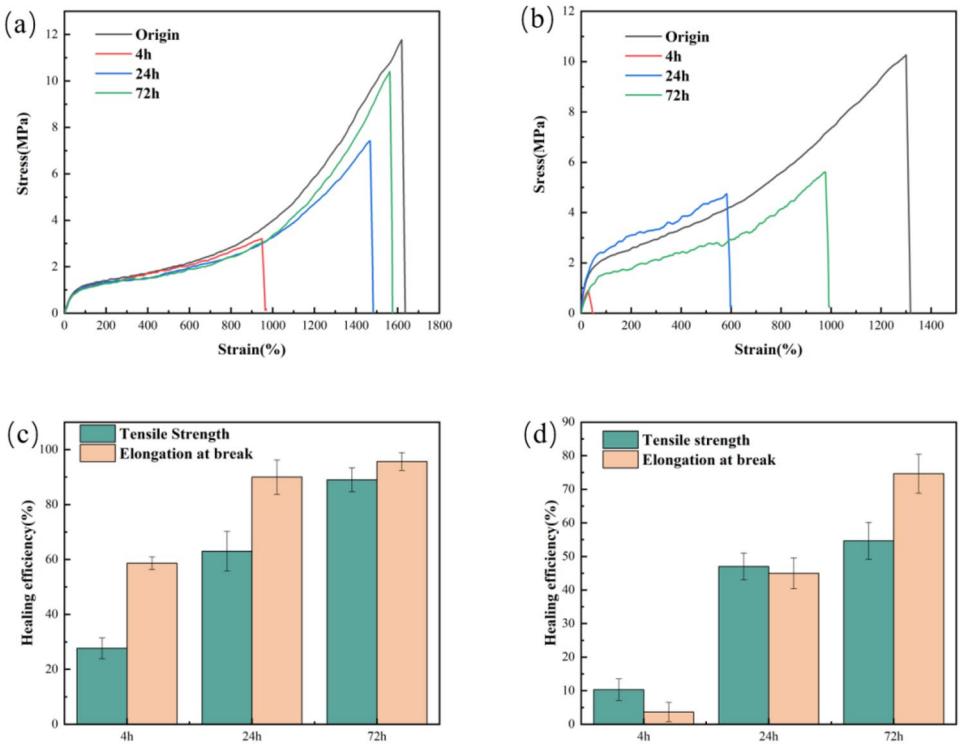

Fig. 10 Stress-strain curves of the original and healed **a** DWPU-$Cu_{0.25,}$ and **b** DWPU-$Cu_{0.5}$; Healing efficiency of DWPU-Cu0.25 (**c**) and DWPU-$Cu_{0.5}$ (**d**)

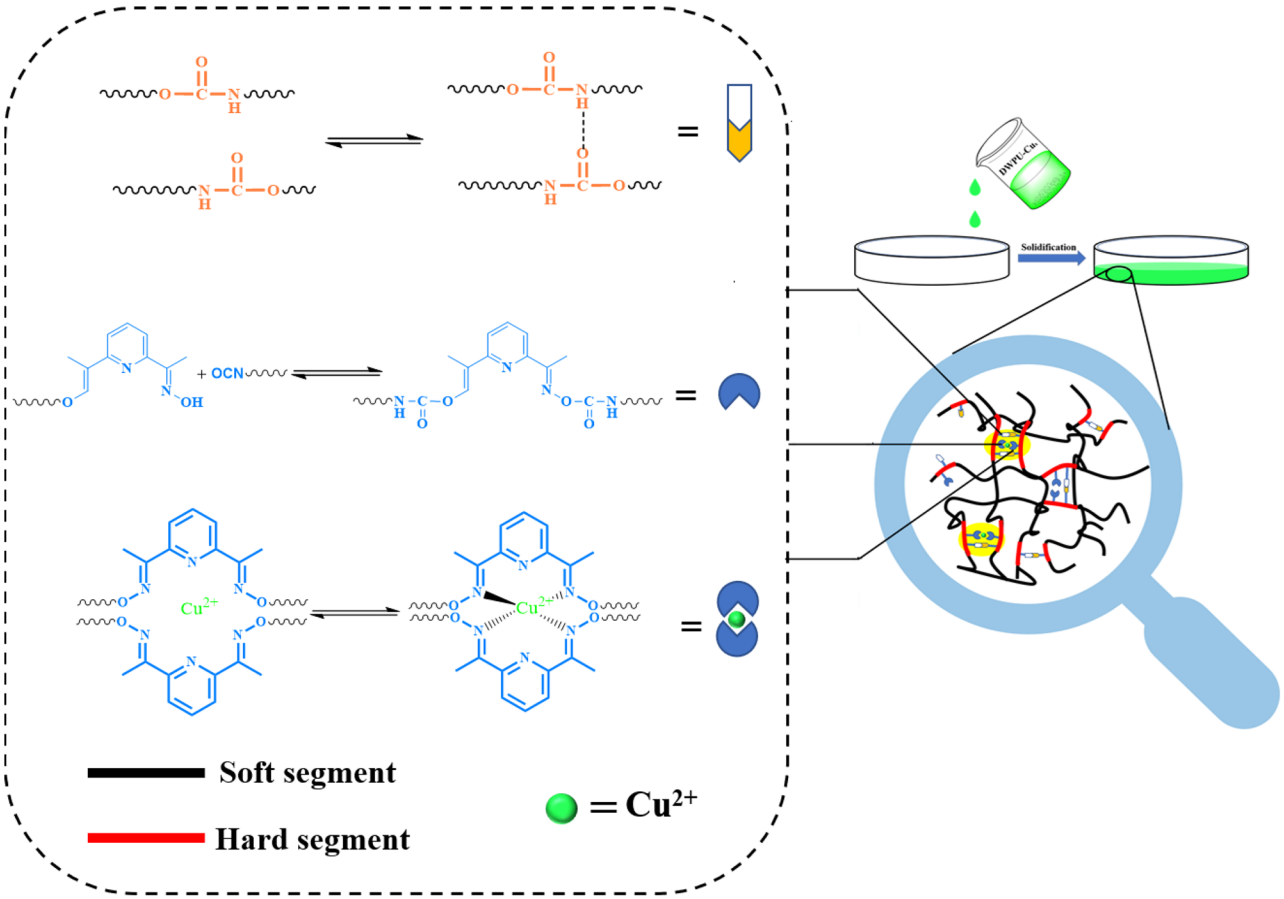

Fig. 11 Schematic diagram of the molecular structure of DWPU-Cu

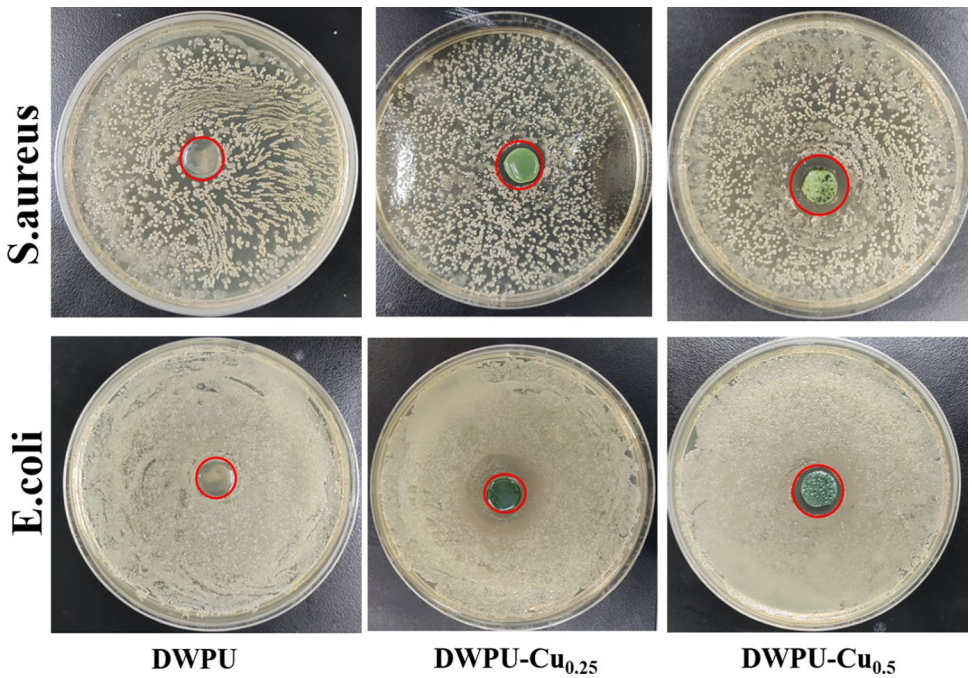

Fig. 12 Composite membrane inhibition circle experiment of DWPU, DWPU-$Cu_{0.25}$, and DWPU-$Cu_{0.5}$

Antimicrobial properties

After adding Cu^{2+}, the modified WPUC has some antibacterial properties in addition to excellent self-healing properties. The results of the inhibition circle experiments are shown in Fig. 12. The results of the inhibition circle experiments revealed that no obvious inhibition zone was observed near the DWPU film without Cu^{2+}, indicating that DWPU did not reflect obvious antibacterial ability on E. coli and S. aureus bacterial Petri dishes. A certain degree of inhibition zone can be observed around the DWPU-Cu0.$_{25}$ and DWPU-$Cu_{0.5}$ composite films. A larger zone of inhibition was observed around the DWPU-$Cu_{0.5}$ composite membrane compared to DWPU-$Cu_{0.25}$, indicating that as the Cu^{2+} content in the polyurethane increased, more Cu^{2+} diffused around the composite membrane, leading to a larger zone of inhibition.

Antimicrobial propertie is mainly due to the direct interaction of copper surface and bacterial outer membrane which also has a small part of Cu2 + caused by toxicity, detailed antibacterial mechanism for bivalent copper ions can directly interact with bacterial cell membrane into the bacterial cell, when the cell copper ion concentration reached a certain value, produce oxidative stress response, lead to intracellular protein and DNA fracture, cell membrane barrier function gradually disappear. Increasing membrane permeability, extravasation of cell contents and inactivation of bacterial cells [45–47].

Conclusions

In this study, we successfully prepared a room temperature self-healing WPU membrane based on multiple dynamic bonds of oxime carbamate bonds, coordination bonds and hydrogen bonds by mixing Cu^{2+} into an aqueous polyurethane emulsion. The mechanical properties of the samples were improved compared to the DWPU without Cu^{2+}. After 72 h at room temperature, the break elongation and tensile strength of the damaged DWPU-$Cu_{0.25}$ returned to 95.8 and 89.1% of the original values, respectively, showing good self-healing ability at room temperature. Moreover, DWPU-Cu also exhibits some antibacterial properties due to the presence of copper ions. Antibacterial experiments showed that DWPU-Cu membrane showed bacterial inhibition against both E. coli and S. aureus. It provides a good idea for the current self-healing of waterborne polyurethane, using a dynamic cross-linked network structure formed by covalent and noncovalent bonds to achieve healing, and introducing metal coordination bonds to enhance the mechanical strength of waterborne polyurethane and give its antibacterial properties by introducing Cu^{2+}. This functional material can extend the service cycle and ensure the safety and stability of polymer components. It has incomparable advantages in expensive equipment and artificial objects that are difficult to repair, meets the needs of new materials for high durability and high stability, and will achieve more functions in the near future.

Supplementary Information The online version contains supplementary material available at https://doi.org/10.1007/s10965-023-03770-y.

Acknowledgements The financial support from the Natural Science Foundation of China (NSFC) (No. 21978112) and MOE & SAFEA for the 111 Project (B13025) is gratefully acknowledged.

Declarations

Conflict of interest The authors declare that have no known competing financial interests or personal relationships that could have appeared to influence the work reported in this paper.

References

1. Liu XH, Hong W, Chen XD (2020) Polymers 12:2875
2. Jia RP, Hui Z, Huang ZX, Liu X, Zhao C, Wang DY, Wu DD (2020) New J Chem 44:19759–19768
3. Kang SY, Ji ZX, Tseng LF, Turner SA, Villanueva DA, Johnson R, Albano A, Langer R (2018) Adv Mater 30:1706237
4. Yang M, Li YC, Dang XG (2022) Environ Res 206:112266
5. Lei L, Zhang YH, Ou CB, Xia ZB, Zhong L (2016) Prog Org Coat 92:85–94
6. Huang SS, Liu GJ, Zhang KK, Hu H, Wang J, Miao L, Tabrizizadeh T (2019) Chem Eng J 360:445–451
7. Chen MX, Li YY, Liu SY, Feng ZX, Wang H, Yang DJ, Guo WM, Yuan ZG, Gao S, Zhang Y, Zha KK, Huang B, Wei F, Sang XY, Tian QY, Yang X, Sui X, Zhou YX, Zheng YF, Guo QY (2021) Bioact Mater 6:1932–1944
8. Zhu MSQ, Liu J, Gan LH, Long MN (2020) Eur Polym J 129:109651
9. Yang HI, Kim DM, Yu HC, Chung CM (2016) ACS Appl Mater Interfaces 8:11070–11075
10. Peng HY, Du XS, Cheng X, Wang HB, Du ZL (2021) Prog Org Coat 151:106081
11. Zhang N, Pan ZC, Li C, Wang J, Jin Y, Song SF, Pan MW, Yuan JF (2022) Polymer 246:124778
12. Han TY, Lin CH, Lin YS, Yeh CM, Chen YA, Li HY, Xiao YT, Chang JW, Su AC, Jeng US, Chou HH (2022) Chem Eng J 438:135592
13. Sheng YM, Wang MH, Zhang KP, Wu ZY, Chen YX, Lu X (2021) Chem Eng J 426:131883
14. Xiao Y, Huang HH, Peng XH (2017) RSC Adv 7:20093–20100
15. Liu J, Tan CSY, Yu ZY, Li N, Abell C, Scherman OA (2017) Adv Mater 29:1605325
16. Mei JF, Jia XY, Lai JC, Sun Y, Li CH, Wu JH, Cao Y, You XZ, Bao ZN (2016) Macromol Rapid Commun 37:1667–1675
17. Burattini S, Greenland BW, Merino DH, Weng WG, Seppala J, Colquhoun HM, Hayes W, Mackay ME, Hamley IW, Rowan SJ (2010) J Am Chem Soc 132:12051–12058
18. Wang ZF, An G, Zhu Y, Liu XM, Chen YH, Wu HK, Wang YJ, Shi XT, Mao CB (2019) Mater Horiz 6:733–742
19. Hou JB, Zhang XQ, Wu D, Feng JF, Ke D, Li BJ, Zhang S (2019) ACS Appl Mater Interfaces 11:12105–12113
20. Peng Y, Yang Y, Wu Q, Wang SX, Huang GS, Wu JR (2018) Polymer 157:172–179

21. Fang YL, Du XS, Jiang YX, Du ZL, Pan PT, Cheng X, Wang HB (2018) ACS Sustain Chem Eng 6:14490–14500
22. Imbernon L, Oikonomou EK, Norvez S, Leibler L (2015) Polym Chem 6:4271–4278
23. Liu MC, Zhong J, Li ZJ, Rong JC, Yang K, Zhou JY, Shen L, Gao F, Huang XL, He HF (2020) Eur Polym J 124:109475
24. Chen Y, Tang ZH, Zhang XH, Liu YJ, Wu SW, Guo BC (2018) ACS Appl Mater Interfaces 10:24224–24231
25. Cash JJ, Kubo T, Bapat AP, Sumerlin BS (2015) Macromolecules 48:2098–2106
26. Xu BW, Han FL, Pei XQ, Zhang SJ, Zhao JB (2021) Ind Eng Chem Res 60:11095–11105
27. Liu XJ, Liu X, Li WJ, Ru Y, Li YH, Sun AL, Wei LH (2021) Chem Eng J 410:128300
28. Li CH, Zuo JL (2020) Adv Mater 32:1903762
29. Zhang WC, Wang MH, Zhou JH, Sheng YM, Xu M, Jiang XL, Ma YH, Lu X (2021) Eur Polym J 156:110614
30. Wang MH, Zhou JH, Jiang XL, Sheng YM, Xu M, Lu X (2021) Eur Polym J 146:110257
31. Zhang LZ, Guan QB, Shen AO, Neisiany RE, You ZW, Zhu MF (2022) Sci China Chem 65:363–372
32. Sai F, Zhang H, Qu J, Wang J, Zhu X, Bai Y, Ye P (2022) Appl Surf Sci 573:151526
33. Mohammadi A, Doctorsafaei AH, Burujeny SB, Rudbari HA, Kordestani N, Ayati SA, Najafabadi (2020) Chem Eng J 381:122776
34. Zhang LZ, Liu ZH, Wu XL, Guan QB, Chen S, Sun LJ, Guo YF, Wang SL, Song JC, Jeffries EM, He CL, Qing FL, Bao XG, You ZW (2019) Adv Mater 31:1901402
35. Liu Y, Li ZJ, Zhang ZT, Wang JC, Sun LY, Xie TL (2021) Prog Org Coat 153:106153
36. Lou WX, Dai ZD, Jiang PP, Zhang PB, Bao YM, Gao XW, Xia JL, Haryono A (2022) Polym Adv Technol 33:2393–2403
37. Wang SY, Ma L, Wang S, Wang YZ, Liu GY, Wang HB (2022) Polym Chem 13:2615–2625
38. Zhu JT, Wu ZM, Xiong D, Pan LS, Liu YJ (2019) Prog Org Coat 133:161–168
39. Li Q, Ma SQ, Wang S, Liu YL, Taher MA, Wang BB, Huang KF, Xu XW, Han YY, Zhu J (2020) Macromolecules 53(4):1474–1485
40. Li Y, Jin Y, Zeng W, Zhou R, Shang X, Shi L, Bai L, Lai C (2023) Prog Org Coat 174:107256
41. Wu XZ, Wang JQ, Huang JX, Yang SR (2019) ACS Appl Mater Interfaces 11:7387–7396
42. Zhang LZ, You ZW (2021) Chin J Polym Sci 39:1281–1291
43. Zhang ZJ, Mei HF, Wang Q, Li R, Wei H, Ouyang X (2022) Mater Chem Phys 285:126070
44. Laxmi A, Shahzaib S, Khan A, Ghosal F, Zafar M, Alam SAA, Nami, Nishat N (2022) J Polym Res 29:152
45. Li QY, Cao L, Wang W, Qin XD, Chen SG (2022) Compos Part A Appl Sci Manuf 163:107213
46. Mirmohseni A, Azizi M, Seyed MS, Dorraji (2019) Prog Org Coat 131:322–332
47. Jiang S, Wang F, Cao X, Slater B, Wang R, Sun H, Wang H, Shen X, Yao Z (2022) Chemosphere 287:132131